In Vivo Imaging of *Caenorhabditis elegans* Glycans

Scott T. Laughlin[†] and Carolyn R. Bertozzi[†,‡,§,⊥,]*

[†]Department of Molecular and Cell Biology, [‡]Department of Chemistry, and [§]Howard Hughes Medical Institute, University of California, Berkeley, California 94720, and [⊥]The Molecular Foundry, Materials Science Division, Lawrence Berkeley National Laboratory, Berkeley, California 94720

ABSTRACT The nematode *Caenorhabditis elegans* is an excellent model organism for studies of glycan dynamics, a goal that requires tools for imaging glycans *in vivo*. Here we applied the bioorthogonal chemical reporter technique for the molecular imaging of mucin-type O-glycans in live *C. elegans*. We treated worms with azido-sugar variants of *N*-acetylglucosamine (GlcNAc), *N*-acetylgalactosamine (GalNAc), and *N*-acetylmannosamine (ManNAc), resulting in the metabolic labeling of their cell-surface glycans with azides. Subsequently, the worms were reacted *via* copper-free click reaction with fluorophore-conjugated difluorinated cyclooctyne (DIFO) reagents. We identified prominent localization of mucins in the pharynx of all four larval stages, in the adult hermaphrodite pharynx, vulva and anus, and in the tail of the adult male. Using a multicolor, time-resolved imaging strategy, we found that the distribution and dynamics of the glycans varied anatomically and with respect to developmental stage.

*Corresponding author,
crb@berkeley.edu.

*C*aenorhabditis elegans glycans are attractive targets for molecular imaging. As a well-established model organism, *C. elegans* offers a system in which to probe the dynamics of glycans in development, disease, and normal physiological processes. Further, glycans have been documented as key players in *C. elegans* biology. For example, vulval morphogenesis and early embryo cytokinesis require the glycosaminoglycan chondroitin sulfate (*1*, *2*). Each stage of *C. elegans* development is associated with specific N-glycan structures, and anatomical features such as the cuticle, vulva, and male tail possess a repertoire of mucin-type O-glycans (*3–5*). Nevertheless, the dynamics of *C. elegans* glycans have remained obscure because they have been inaccessible to analysis by molecular imaging.

Here we applied the bioorthogonal chemical reporter strategy (*6*), which we recently described for imaging glycans in developing zebrafish (*7*), to the molecular imaging of glycans in live *C. elegans*. In the first step, we metabolically incorporate an azidosugar into the worm's glycans by using their own biosynthetic machinery (Figure 1, panel a). Per-*O*-acetylated azidosugars passively diffuse into the cells where their hydroxyl groups are deacetylated by promiscuous intracellular esterases (*8*). The free sugar is processed and integrated into newly synthesized glycans, some of which are displayed on cell-surface glycoconjugates. The azidosugars are then imaged in a second step with difluorinated cyclooctyne (DIFO)-based probes (Figure 1, panel b) *via* copper-free click chemistry (*9*).

Additionally, azide-labeled glycoconjugates can be analyzed *ex vivo* by reaction of tissue lysates with alkyne- or triarylphosphine-based probes (*e.g.*, *via* the Staudinger ligation (*10*)) followed by Western blot.

Because the metabolism of azidosugars in nonvertebrate animals has not been tested, we first assayed the ability of *C. elegans* to incorporate azido analogues of ManNAc, GalNAc, and GlcNAc into glycoproteins. We seeded nematode growth medium (NGM)-agar plates containing 1 mM per-*O*-acetylated *N*-azidoacetylmannosamine (Ac$_4$ManNAz), -galactosamine (Ac$_4$GalNAz), or -glucosamine (Ac$_4$GlcNAz) with 10 larval (L1) wild-type *C. elegans* (strain N2). We allowed the population of worms to expand until the bacterial food source was consumed. Then, we made lysates from the mixed-stage population of worms, reacted them with phosphine-Flag, and analyzed the resident glycoproteins for the presence of azides using standard Western blot techniques (Figure 1, panel c). We observed robust incorporation of GalNAz into glycoproteins, indicating that *C. elegans*' metabolic enzymes are tolerant of this azidosugar. Samples from Ac$_4$GlcNAz- and Ac$_4$ManNAz-treated worms produced no observable signal in the Western blot, indicating that these azidosugars are not incorporated into *C. elegans* glycans at significant levels. This was not unexpected because, in mammalian cells, GlcNAz is incorporated into cytosolic *O*-GlcNAcylated proteins at low levels with no significant cell-surface glycoprotein labeling (*11*). ManNAz is converted by mammalian cells to the corre-

sponding azido sialic acid (*10*), a residue that is absent in *C. elegans* (*12*).

We sought to determine the types of glycoproteins being labeled by Ac$_4$GalNAz. The naturally occurring counterpart of GalNAz, GalNAc, is found in mucin-type O-glycans (*13*), chondroitin sulfate (*14*), and rarely, N-glycans (*15*). In order to probe for GalNAz residues within chondroitin sulfate and N-glycans, we reacted lysates from Ac$_4$GalNAz-treated *C. elegans* with chondroitinase ABC or peptide *N*-glycosidase F (PNGase F), enzymes that digest the respective glycans. Then, we reacted the enzyme-treated lysates with phosphine-Flag and probed the glycoproteins by Western blotting with an α-Flag antibody. Neither enzyme-treated sample showed a significant decrease in chemiluminescence signal compared to undigested lysate (Supplementary Figure 1a,b), indicating that a majority of GalNAz residues are situated in other types of glycans.

We recently found that mammalian cells epimerize the nucleotide sugar derived from GalNAz, uridine diphosphatidyl (UDP)-GalNAz, to UDP-GlcNAz and that the enzyme O-GlcNAc transferase (OGT) further installs the azidosugar on nuclear and cytoplasmic proteins that would normally be O-GlcNAcylated (*16*). In order to determine if this phenomenon occurs in worms, we treated an OGT-deficient *C. elegans* strain, RB653 (*17*), with Ac$_4$GalNAz. Western blots of phosphine-Flag-labeled lysates from Ac$_4$GalNAz-treated RB653 worms were indistinguishable from similarly treated wild-type samples (Supplementary Figure 1c). This observation suggests that GalNAz does not metabolically label O-GlcNAcylated proteins appreciably in this organism.

Finally, we probed the binding of the azide-labeled glycoproteins to lectins specific for N- or O-glycans. We observed no detectable binding of azide-labeled glycoproteins to the N-glycan specific lectin concanavalin A (ConA), consistent with
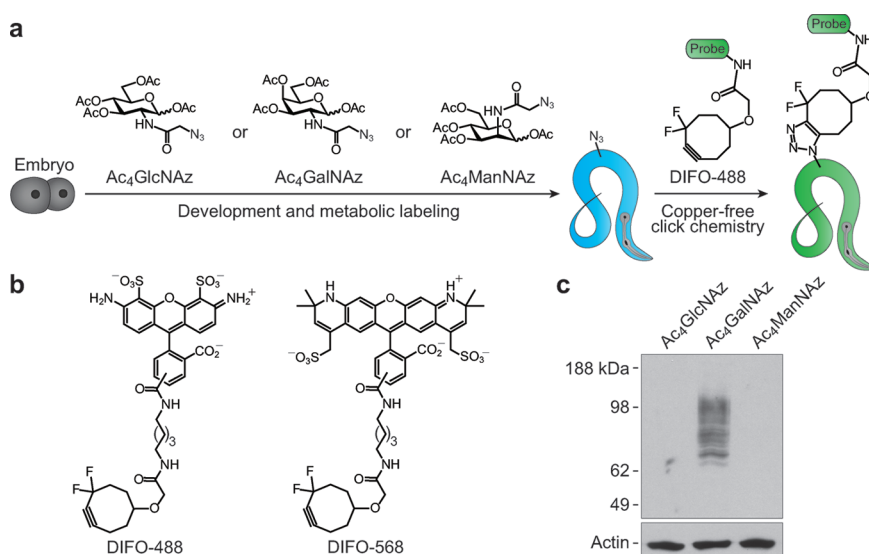

Figure 1. A bioorthogonal chemical reporter strategy for *in vivo* imaging of glycans in *C. elegans*. a) *C. elegans* embryos metabolize azidosugars and incorporate them into newly synthesized cell-surface glycans (blue). Copper-free click chemistry with fluorophore-conjugated difluorinated cyclooctyne (DIFO) reagents (green) enables imaging of glycans by fluorescence microscopy. **b)** The DIFO-488 and -568 probes used in this study. **c)** Lysates from mixed-stage *C. elegans* that had been incubated with Ac$_4$GlcNAz, Ac$_4$GalNAz, or Ac$_4$ManNAz were reacted with phosphine-Flag and subsequently analyzed by Western blot, probing with HRP-conjugated α-Flag clone M2 (top panel) or mouse α-actin (bottom panel).

the hypothesis that a majority of labeled glycans are O-linked. Moreover, a small fraction of GalNAz-labeled species were retained on peanut agglutinin (PNA)-conjugated agarose beads, and judging by the faint chemiluminescence signal of the relevant phosphine-Flag-modified sample, some of them were selectively eluted with galactose (Supplementary Figure 2). These results indicate that only a subset of GalNAz-labeled glycoproteins possess the unmodified form of the core 1 O-glycan, galactoseβ1–3GalNAc, which is recognized by PNA (*18*). That only a fraction of GalNAz-labeled glycoproteins bound to PNA-agarose was not unexpected because *C. elegans* O-glycans possess extended peripheral structures that would mask the PNA epitope (*19*).

Collectively, our *in vitro* characterization experiments suggest that GalNAz is incorporated into mucin-type O-glycans in *C. ele-*

gans. We should note, however, that Western blot analysis of lysates does not probe glycolipids, which may possess GalNAc residues (*20*), nor does the technique analyze those species that are not soluble in the detergent lysis buffer. Thus, we cannot rule out the possibility that other glycans, such as insoluble cuticle-associated chondroitin sulfate proteoglycans (*21*), are metabolically labeled with GalNAz.

We next sought to image the azide-labeled glycans in live *C. elegans* in order to reveal their anatomical distribution at different stages of development. To accomplish this, we employed copper-free click chemistry using an Alexa Fluor 488-conjugated DIFO reagent termed DIFO-488 (*9*). Strains N2 or CA151 were grown with or without 5 mM Ac$_4$GalNAz as described above. The CA151 strain contains a *him*-8 (high incidence of males) mutation that impairs X chromosome segregation, resulting
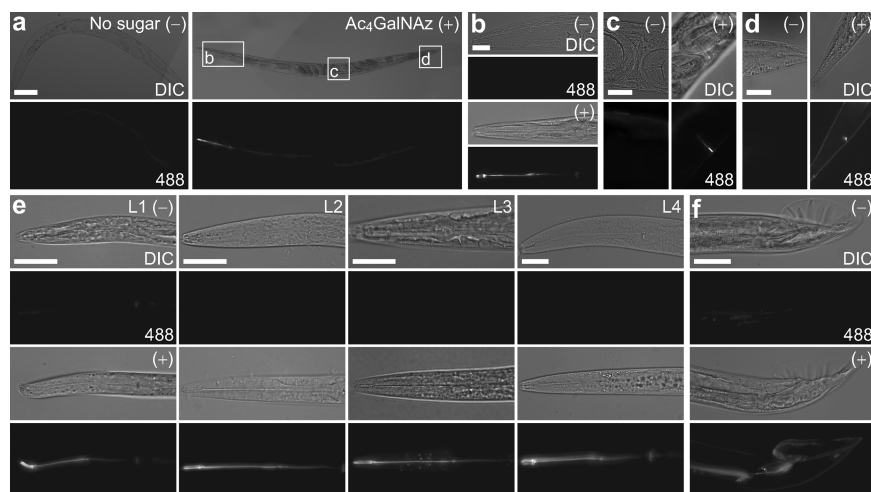
Figure 2. *In vivo* imaging of glycan distribution in larval and adult *C. elegans*. a) *C. elegans* adult hermaphrodites that had been incubated with Ac$_4$GalNAz (+) or no sugar (−) were reacted with DIFO-488 and imaged alive. Fluorescence was observed in the pharynx (b), vulva (c), and anus (d) of Ac$_4$GalNAz-treated (+) but not in the no sugar control (−) worms. b–d) Higher magnification images of the pharynx (b), vulva (c), and anus (d) regions. e) *C. elegans* hermaphrodites at larval stage L1−L4 that had been incubated with Ac$_4$GalNAz (+) or no sugar (−) were reacted with DIFO-488. Fluorescence was observed in the pharynx region of Ac$_4$GalNAz-treated worms. f) *C. elegans* strain CA151 adult males metabolically labeled with Ac$_4$GalNAz (+) or no sugar (−) were reacted with DIFO-488. Fluorescence was observed in the tail region of Ac$_4$GalNAz-treated worms. DIC denotes differential interference contrast. 488 denotes DIFO-488 fluorescence. Scale bars: (a) 100 μm; (b–f) 25 μm.

in the production of 40% male worms (compared to the wild-type occurrence of 0.1%) and thus allows the visualization of male-specific structures (*22*).

Mixed-stage populations of Ac$_4$GalNAz-treated or untreated ("no sugar") *C. elegans* were reacted with DIFO-488 for 1 h, washed briefly, and then anesthetized prior to imaging (Figure 2). In the adult hermaphrodite, we observed GalNAz-specific labeling in the pharynx, vulva, and anus (Figure 2, panels a–d). The labeled glycans were concentrated in the pharynx of all larval and adult worms (Figure 2, panels a, b, e), though higher exposure times did reveal some staining of the worms' outer coat, the cuticle (Figure 2, panel d). Like the adult hermaphrodites, the adult males stained intensely in the pharynx region and minimally in the anus and cuticle. However, the male tail also showed striking labeling of the fan, spicule, and rays (Figure 2, panel f). Since

the *C. elegans* cuticle is notoriously impenetrable by small molecules (*23*), we suspect that Ac$_4$GalNAz enters the worm by ingestion. The intense fluorescence observed in the pharynx is consistent with this presumption. Control worms that were not incubated with azidosugar showed minimal background fluorescence, and neither azidosugar metabolism nor DIFO-488 labeling produced observable toxicity. Importantly, the observed fluorescence is not due to *Escherichia coli* reacting with DIFO-conjugates and adhering to the worms. *E. coli* were visible in high magnification images next to worms and were not labeled with DIFO-fluorophore conjugates (Supplementary Figure 3).

The one-color labeling protocol enabled the visualization of the GalNAz-containing glycans that were produced throughout *C. elegans* larval development and into adulthood; however, this strategy does not

highlight nascent glycans, as would be necessary to study their dynamics. To identify "hot spots" of O-glycan biosynthesis, we employed a two-color labeling strategy (Figure 3, panel a). We metabolically labeled mixed-stage strains N2 and CA151 with Ac$_4$GalNAz and then reacted the worms with DIFO-488 as described above. We then transferred the specimens back to plates containing Ac$_4$GalNAz (or to control plates) for an additional 12 h. During this second incubation, only the newly synthesized glycans were metabolically labeled with GalNAz. We reacted these worms with Alexa Fluor 568-conjugated DIFO (DIFO-568, Figure 1, panel b). Thus, at the end of the two labeling steps, the older population of glycans should be labeled with DIFO-488 (false-colored green) and the newer glycans with DIFO-568 (false-colored red). The anatomical distributions of the two dyes at various developmental stages were then analyzed by fluorescence imaging of live anesthetized worms.

Figure 3, panel b shows two-color fluorescence images of worms at three different developmental stages: L1, L2, and adult. Worms in the first larval stage (L1) when the image was acquired would have been eggs at the time of the initial labeling reaction. Accordingly, these worms show no labeling with DIFO-488 (green) but intense labeling with DIFO-568 (red), which was administered 12 h later (Figure 3, panel b, top row). By contrast, worms in the second larval stage (L2) when the image was acquired were in stage L1 during the DIFO-488 labeling reaction. These worms display roughly equal and overlapping green and red fluorescence, indicating that O-glycans were produced in the same anatomical regions during the first two larval stages. One region of the L2 larvae labeled more intensely with DIFO-568 (red) than with DIFO-488: the posterior pharynx (also called the "grinder," marked in Figure 3, panel b by arrowheads). This local increase in the production of O-glycans was even more pro-

nounced in adult worms (Figure 3, panel b, marked by arrowheads).

In the adult vulva, the products from both labeling reactions were apparent, though the DIFO-568 fluorescence signal was less intense. The limited fluorescence associated with new glycans indicates that O-glycan biosynthesis occurred at relatively low levels in the vulva of adult hermaphrodites (Figure 3, panel c). In the male sex organs, we observed intense DIFO-488 labeling of the fan but minimal DIFO-568 labeling. Rather, the DIFO-568 highlighted the spicule and cloaca, indicating that new glycans are continually produced in these areas in the adult worm (Figure 3, panel d). These components of the male sex organs are known to have motive capabilities (24), a property shared with the pharynx (25). It is possible that mucin-type O-glycan production is required to supply lubricating mucin glycoproteins for these processes (26). Also, the organs most readily labeled with DIFO probes are those that are accessible to solution (*i.e.*, pharynx, vulva, and male tail). This observation most likely reflects the Alexa Fluor probes' limited penetrance into the organism. Thus, an important area of future optimization involves the development of fluorescent dyes capable of greater dissemination among the tissues of live worms.

In conclusion, we demonstrated that O-glycans can be imaged in live *C. elegans*, enabling studies of their distribution and dynamics from larvae to adulthood in both hermaphrodites and males. The technique may also have utility in other studies of *C. elegans* glycobiology that would benefit from spatial and temporal resolution, such as pathogenesis or aging.

METHODS

Materials and General Methods. All chemicals were of analytical grade, obtained from commercial suppliers, and used without further purification. Phosphine-Flag, DIFO-488, DIFO-568, Ac$_4$GalNAz, Ac$_4$ManNAz, and Ac$_4$GlcNAz were synthesized as previously described (9, 16, 27). *C. elegans* strains N2, CA151, and RB653 were ob-
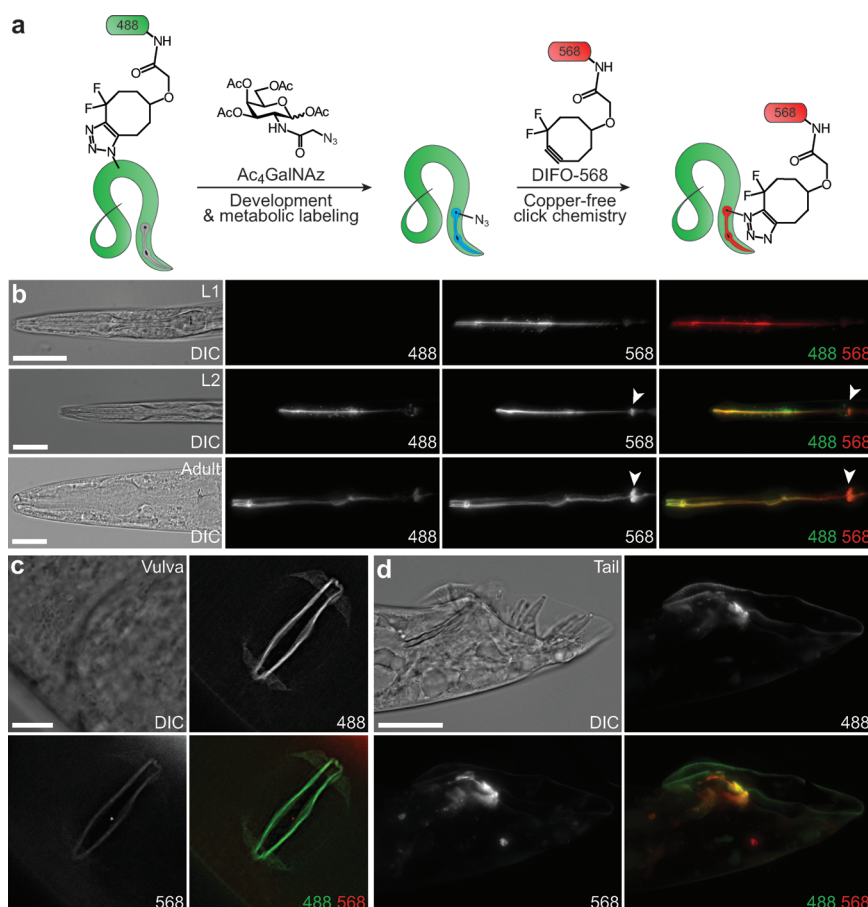

Figure 3. Two-color imaging of nascent glycans in live *C. elegans*. a) *C. elegans* embryos that were previously labeled with Ac$_4$GalNAz and reacted with DIFO-488 (green) were incubated again with Ac$_4$GalNAz to metabolically label a second, newer population of glycans with azides (blue). These newly labeled glycans were then reacted with DIFO-568 (red) to distinguish the old from the new populations. b) L1 (top panels), L2 (middle panels), or adult (bottom panels) *C. elegans* metabolically labeled with Ac$_4$GalNAz were reacted with DIFO-488 and DIFO-568 as described in panel a. Arrowheads denote the "grinder" in the anterior pharynx region. c, d) Strain N2 adult hermaphrodite (c) or strain CA151 adult male (d) *C. elegans* that were metabolically labeled with Ac$_4$GalNAz were reacted with DIFO-488 and DIFO-568 as described in panel a. DIC denotes differential interference contrast, 488 denotes DIFO-488 fluorescence, and 568 denotes DIFO-568 fluorescence. Scale bars: (b, d) 25 μm; (c) 10 μm.

tained from the *C. elegans* Genetics Center. α-Actin clone C4 was obtained from AbCAM. Phosphate-buffered saline solution without calcium and magnesium (PBS) and SeeBlue Plus2 prestained protein molecular weight markers were obtained from Invitrogen Life Technologies, Inc. Nematode growth media (NGM) was obtained from United States Biological. Complete mini protease inhibitor tablets with ethylene diamine tetraacetic acid (EDTA) were obtained from Roche Applied Biosciences. Bis-Tris polyacrylamide gels and the detergent-compatible (DC) protein assay kit were obtained from Bio-Rad. HRP-conjugated α-mouse IgG was obtained from Jackson ImmunoResearch Laboratories. Peptide *N*-glycosidase F (PNGase F) was obtained from New England Biolabs. Restore Western blot stripping buffer and SuperSignal West Pico chemiluminescent substrate were obtained from Pierce Biotechnology. α-Chondroitin sulfate ΔDi-Os was obtained from Seikagaku Corporation. Chondroitinase ABC from *Proteus vulgaris*, HRP-conjugated α-Flag clone M2, Nonidet P 40 Substitute, Ponceau S, and RNase B were obtained from Sigma-Aldrich.

C. elegans disruption was performed with a Misonix Sonicator 3000 equipped with a microprobe. Images were acquired with a Zeiss Axiovert 200 M deconvolution microscope, deconvolved using the nearest neighbor deconvolution algorithm of Slidebook (Intelligent Imaging Innovations), and displayed as a maximum intensity projection of the Z-axis.

Labeling C. elegans Glycans with Azidosugars. Wild-type (strain N2), him-8(me4) mutants (strain CA151), and ogt mutants (strain RB653) were maintained on NGM agar plates with E. coli (strain OP50) at 21 °C. For metabolic labeling experiments, a 10-cm Petri dish containing NGM plus 1 mM (Western blot experiments) or 5 mM (imaging experiments) of $Ac_4GlcNAz$, $Ac_4GalNAz$, $Ac_4ManNAz$, or negative control was inoculated with 100 μL of an OP50 culture that had an optical density at 600 nm (OD_{600}) of 50, and these plates were grown for 24 h at 37 °C. To each plate were added 10 L1 C. elegans of the appropriate strain and the population was grown at 21 °C for 8 d, or until the bacterial lawn was consumed.

Phosphine-Flag Reaction with C. elegans Lysates. $Ac_4GlcNAz$-, $Ac_4GalNAz$-, $Ac_4ManNAz$-, or negative control-treated mixed-staged C. elegans were washed from the NGM agar plate with 4×2.5 mL PBS into a 15-mL centrifuge tube. The worms were concentrated by centrifugation ($100 \times g$, 3 min, 4 °C), the supernatant was removed, and 10 mL of PBS was added. This wash process was repeated twice more for a total of three washes. The washed worms were then transferred to a 1.5-mL eppendorf tube and concentrated by centrifugation ($100 \times g$, 3 min, 4 °C), the supernatant was removed, and 200 μL of ice cold lysis buffer was added (150 mM NaCl, 20 mM Tris pH 7.4, 1% Nonidet P 40 Substitute, and one Roche complete mini protease inhibitor tablet with EDTA for every 10 mL of lysis buffer). The worms were disrupted by sonication on ice with 30-s, ~9-W pulses three times, and then insoluble debris was removed by centrifugation ($16,000 \times g$, 10 min, 4 °C). The protein concentration was determined using the Bio-RAD DC protein assay. Ten micrograms of total protein from these lysates were reacted for 12 h at 21 °C with 250 μM Phosphine-Flag and subsequently assayed using standard Western blot procedures, probing with a 1:5000 dilution of HRP-conjugated α-Flag clone M2.

Live Imaging of GalNAz-Labeled C. elegans. Mixed-stage strain N2 or CA151 C. elegans that had been metabolically labeled with 5 mM $Ac_4GalNAz$ were reacted with 100 μL of 100 μM DIFO-488 in PBS for 1 h at 21 °C. After 1 h, the reaction was quenched by dilution to 10 mL with PBS. The worms were washed by centrifugation six times in 10 mL PBS ($100 \times g$, 3 min, 4 °C). For the one-color imaging experiments, the worms were anesthetized with 10 mM NaN_3 and imaged with a Zeiss Axiovert 200 M deconvolution microscope. For the two-color imaging experiments, the worms were transferred from the final PBS wash to 10-cm NGM plates containing 5 mM $Ac_4GalNAz$ or no sugar as a negative control. After 12 h, the worms were reacted with 100 μL of 100 μM DIFO-

568 in PBS for 1 h at 21 °C, washed, and imaged as described above for the one-color experiment.

REFERENCES

1. Hwang, H. Y., Olson, S. K., Esko, J. D., and Horvitz, H. R. (2003) *Caenorhabditis elegans* early embryogenesis and vulval morphogenesis require chondroitin biosynthesis, *Nature 423*, 439–443.
2. Mizuguchi, S., Uyama, T., Kitagawa, H., Nomura, K. H., Dejima, K., Gengyo-Ando, K., Mitani, S., Sugahara, K., and Nomura, K. (2003) Chondroitin proteoglycans are involved in cell division of *Caenorhabditis elegans*, *Nature 423*, 443–448.
3. Natsuka, S., Adachi, J., Kawaguchi, M., Nakakita, S., Hase, S., Ichikawa, A., and Ikura, K. (2002) Structural analysis of N-linked glycans in *Caenorhabditis elegans*, *J. Biochem. 131*, 807–813.
4. Link, C. D., Ehrenfels, C. W., and Wood, W. B. (1988) Mutant expression of male copulatory bursa surface markers in *Caenorhabditis elegans*, *Development 103*, 485–495.
5. Link, C. D., Silverman, M. A., Breen, M., Watt, K. E., and Dames, S. A. (1992) Characterization of *Caenorhabditis elegans* lectin-binding mutants, *Genetics 131*, 867–881.
6. Laughlin, S. T., and Bertozzi, C. R. (2008) Imaging the glycome, *Proc. Natl. Acad. Sci. U.S.A. 106*, 12–17.
7. Laughlin, S. T., Baskin, J. M., Amacher, S. L., and Bertozzi, C. R. (2008) *In vivo* imaging of membrane-associated glycans in developing zebrafish, *Science 320*, 664–667.
8. Luchansky, S. J., Goon, S., and Bertozzi, C. R. (2004) Expanding the diversity of unnatural cell-surface sialic acids, *ChemBioChem 5*, 371–374.
9. Baskin, J. M., Prescher, J. A., Laughlin, S. T., Agard, N. J., Chang, P. V., Miller, I. A., Lo, A., Codelli, J. A., and Bertozzi, C. R. (2007) Copper-free click chemistry for dynamic *in vivo* imaging, *Proc. Natl. Acad. Sci. U.S.A. 104*, 16793–16797.
10. Saxon, E., and Bertozzi, C. R. (2000) Cell surface engineering by a modified Staudinger reaction, *Science 287*, 2007–2010.
11. Vocadlo, D. J., Hang, H. C., Kim, E. J., Hanover, J. A., and Bertozzi, C. R. (2003) A chemical approach for identifying O-GlcNAc-modified proteins in cells, *Proc. Natl. Acad. Sci. U.S.A. 100*, 9116–9121.
12. Bacic, A., Kahane, I., and Zuckerman, B. M. (1990) Panagrellus redivivus and *Caenorhabditis elegans*: evidence for the absence of sialic acids, *Exp. Parasitol. 71*, 483–488.
13. Hang, H. C., and Bertozzi, C. R. (2005) The chemistry and biology of mucin-type O-linked glycosylation, *Bioorg. Med. Chem. 13*, 5021–5034.
14. Silbert, J. E., and Sugumaran, G. (2002) Biosynthesis of chondroitin/dermatan sulfate, *IUBMB Life 54*, 177–186.
15. Kawar, Z. S., Van Die, I., and Cummings, R. D. (2002) Molecular cloning and enzymatic characterization of a UDP-GalNAc:GlcNAc(β)-R β1,4-N-acetylgalactosaminyltransferase from *Caenorhabditis elegans*, *J. Biol. Chem. 277*, 34924–34932.
16. Laughlin, S. T., and Bertozzi, C. R. (2007) Metabolic labeling of glycans with azido sugars and subsequent glycan-profiling and visualization via Staudinger ligation, *Nat. Protoc. 2*, 2930–2944.
17. Hanover, J. A., Forsythe, M. E., Hennessey, P. T., Brodigan, T. M., Love, D. C., Ashwell, G., and Krause, M. (2005) A *Caenorhabditis elegans* model of insulin resistance: altered macronutrient storage and dauer formation in an OGT-1 knockout, *Proc. Natl. Acad. Sci. U.S.A. 102*, 11266–11271.
18. Iskratsch, T., Braun, A., Paschinger, K., and Wilson, I. B. H. (2009) Specificity analysis of lectins and antibodies using remodeled glycoproteins, *Anal. Biochem. 386*, 133–146.
19. Guerardel, Y., Balanzino, L., Maes, E., Leroy, Y., Coddeville, B., Oriol, R., and Strecker, G. (2001) The nematode *Caenorhabditis elegans* synthesizes unusual O-linked glycans: identification of glucose-substituted mucin-type O-glycans and short chondroitin-like oligosaccharides, *Biochem. J. 357*, 167–182.
20. Wu, A. M. (2002) Carbohydrate structural units in glycosphingolipids as receptors for Gal and GalNAc reactive lectins, *Neurochem. Res. 27*, 593–600.
21. Peixoto, C. A., and De Souza, W. (1992) Cytochemical characterization of the cuticle of *Caenorhabditis elegans* (Nematoda: Rhabditoidea), *J. Submicrosc. Cytol. Pathol. 24*, 425–435.
22. Phillips, C. M., Wong, C., Bhalla, N., Carlton, P. M., Weiser, P., Meneely, P. M., and Dernburg, A. F. (2005) HIM-8 binds to the X chromosome pairing center and mediates chromosome-specific meiotic synapsis, *Cell 123*, 1051–1063.
23. Segalat, L. (2007) Invertebrate animal models of diseases as screening tools in drug discovery, *ACS Chem. Biol. 2*, 231–236.
24. Emmons, S. W., Sternberg, P. W. (1997) Male development and mating behavior. In *C. elegans II* (Riddle, D. L., Blumenthal, T., Meyer, B. J., Priess J. R., Eds.), pp 295–334, Cold Spring Harbor Laboratory Press, New York.
25. Avery, L., Thomas, J. H. (1997) Feeding and defecation. In *C. elegans II* (Riddle, D. L., Blumenthal, T. Meyer, B. J., Priess, J. R., Eds.), pp 679–716, Cold Spring Harbor Laboratory Press, New York.
26. Yakubov, G. E., McColl, J., Bongaerts, J. H., and Ramsden, J. J. (2009) Viscous boundary lubrication of hydrophobic surfaces by mucin, *Langmuir 25*, 2313–2321.
27. Laughlin, S. T., Agard, N. J., Baskin, J. M., Carrico, I. S., Chang, P. V., Ganguli, A. S., Hangauer, M. J., Lo, A., Prescher, J. A., and Bertozzi, C. R. (2006) Metabolic labeling of glycans with azido sugars for visualization and glycoproteomics, *Methods Enzymol. 415*, 230–250.